Magnetic properties of the diluted magnetic semiconductor $Zn_{1-x}Fe_xSe$

H. J. M. Swagten, A. Twardowski,* and W. J. M. de Jonge
Eindhoven University of Technology, Department of Physics, P.O. Box 513, 5600 MB Eindhoven, The Netherlands

M. Demianiuk
Institute of Technical Physics, Wojskowa Akademia Techniczna, 00908 Warsaw, Poland
(Received 4 May 1988)

The magnetic specific heat and low-field ac susceptibility of the iron-based diluted magnetic semiconductor (DMS) $Zn_{1-x}Fe_xSe$ in the temperature range 0.4–20 K are reported. Antiferromagnetic *d-d* interactions and indications of spin-glass freezing are observed. These data, together with high-temperature susceptibility and high-field magnetization, are interpreted in the extended nearest-neighbor pair approximation, with an antiferromagnetic exchange between the Fe^{2+} ions. Fair agreement between theory and experiment is obtained for all the thermodynamic quantities with one set of parameters provided by independent experiments. The strength and range of the interactions, as well as the freezing mechanisms, are compared with DMS's containing Mn^{2+}, and the results are discussed in relation with the existing models.

I. INTRODUCTION

Diluted magnetic semiconductors (DMS's) or semimagnetic semiconductors (SMSC's)—i.e., II-VI, II-V, or IV-VI semiconductors with a controlled amount of magnetic ions substituted for nonmagnetic cations—have been extensively studied during the recent years because of their interesting magneto-optical and magnetic properties.[1] Since DMS's can generally be synthesized with a wide range of concentrations of magnetic ions, they offer an exceptional possibility to study both the very diluted and the concentrated regimes in one material. In fact, the existence of paramagnetic, spin-glass, and antiferromagnetic phases was reported in these materials depending on the concentration and temperature range.[1]

So far the research has been devoted mainly to DMS's containing Mn ions. The magnetic behavior of these systems show common characteristics which can be understood on the basis of a random array of localized Mn ions coupled by long ranged, isotropic antiferromagnetic exchange interactions[1–3] which are mediated by the carriers. The underlying microscopic mechanisms in relation to the band structure, as well as the nature of and the driving force behind the observed phase transition and the role of the anisotropy, are, however, still somewhat obscure and an object of further investigations.[2,3]

In that respect, substitutional Mn^{2+} with its degenerate $^6A_1$ spin-only ground state represents a rather simple, although theoretically attractive, case since all the phenomena which involve orbital momentum are absent.

In contrast,substitutional iron Fe^{2+} can serve as a much more general case, since it possesses both spin and orbital momenta ($S=2$ and $L=2$). Iron Fe^{2+} has a d^6 electronic configuration. The ground state of a Fe^{2+} free ion (^5D) is splitted by a tetrahedral crystal field into a ^5E orbital doublet and a higher-lying ^5T orbital triplet (separated from ^5E by $\Delta=10Dq$, where Dq is crystal-field parameter). The spin-orbit interaction splits the ^5E term into a singlet A_1, a triplet T_1, a doublet E, a triplet T_2, and a singlet A_2 (the energy separation between these states is approximately equal to $6\lambda^2/10Dq$, where λ is the spin-orbit parameter).[4,5] The ground state is a magnetically inactive singlet A_1 resulting in Van Vleck–type paramagnetism.[4–6] The properties of Fe-based DMS's are, however, relatively unexplored yet,[7] although recently some attempts to understand the magnetic behavior of these compounds were reported.[8–11] In view of that, we thought it worthwhile to study the magnetic properties of $Zn_{1-x}Fe_xSe$ in some detail.

In this paper we report the results of magnetic specific heat and low-field susceptibility measurements in the temperature range 0.4–20 K. Together with the high-temperature susceptibility obtained by us[11] very recently, and high-field magnetization data,[8] we were able—for the first time for Fe-based DMS's—to describe all these magnetic properties within one model (extended nearest-neighbor pair approximation) and obtain a fairly good agreement between experiment and theory.

II. EXPERIMENTAL RESULTS

The samples of $Zn_{1-x}Fe_xSe$ were grown by the modified Bridgman method under the pressure of a neutral gas, in the nominal concentration range $0.001<x<0.55$. All the ingots were checked by microprobe analysis and it was found that the iron concentration never exceeded $x=0.22$. Growing crystals with higher iron content only yielded an increase of precipitations of iron selenide. Crystals with precipitations were not used for further study.

The crystalline structure of this material was studied by x-ray diffraction and was found to be cubic in the whole concentration range. Variation of the resulting lattice constant with x is shown in Fig. 1. Results reported for $Zn_{1-x}Fe_xSe$ thin layers[12] are also inserted in this figure.

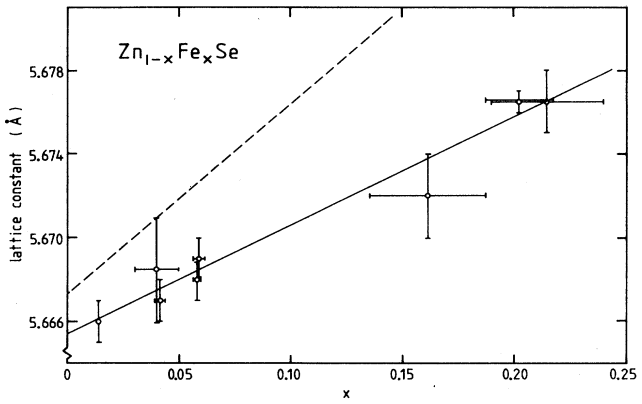

FIG. 1. Lattice constant of $Zn_{1-x}Fe_xSe$ as a function of concentration x. The solid line denoting $a(x)=(5.666\pm0.001)+(0.051\pm0.01)x$ Å is obtained from a least-squares fit. The dashed line represents results from Ref. 12.

The electron paramagnetic resonance (EPR) analysis performed on some of our samples revealed the presence of paramagnetic impurities (mainly Mn^{2+}) originating from the source materials used for crystal growing. The concentration of these impurities was typically less than 0.01% of the actual Fe^{2+} content. The Fe concentration of the crystals reported in this paper was $x=0.014$, 0.04, 0.062, and 0.14, and 0.21.

A. Low-temperature susceptibility

The ac susceptibility χ was measured with a conventional mutual inductance bridge operating in the region 100 Hz $<f<$ 2000 Hz and fields less than 0.0001 T. Some representative susceptibility data are shown in Fig. 2. The data for low concentrations ($x<0.07$) differ from susceptibility results previously reported for Fe^{2+}-doped crystals[6]: instead of temperature-independent susceptibility at low temperatures (i.e., typical Van Vleck–type paramagnetism), we observe a monotonous increase of the susceptibility. We believe that such a behavior is due to paramagnetic impurities present in our crystals, as mentioned earlier. We estimated this additional contribution to χ as a difference between the χ value at 4 K and χ measured below 4 K. For $Zn_{0.958}Fe_{0.042}Se$, the Mn^{2+} impurity concentration was estimated this way as $x_{imp}=0.0002$, in fair agreement with EPR data for this crystal. For the crystals with higher x, one can observe a maximum in χ, which is well pronounced for $x=0.21$ at $T_f=9$ K, whereas for $x=0.144$, one can only notice that it appears at roughly 2 K. Since no anomalies occur in the specific heat for these samples at the corresponding temperatures, we tentatively ascribe these maxima to a paramagnetic-spin-glass phase transition, in analogy with the Mn systems. We should stress however, that this conjecture requires further study. In particular the zero-field-cooled and field-cooled dc susceptibility should be measured, and a wider composition range should be investigated. The latter one depends, however, strongly on improvement in the crystal growing technology.

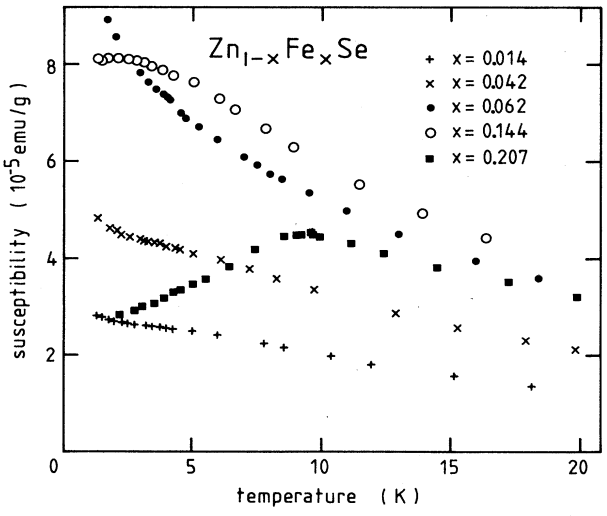

FIG. 2. ac susceptibility of $Zn_{1-x}Fe_xSe$ as a function of temperature.

Nevertheless, if one accepts the nature of the susceptibility anomaly as a spin-glass freezing, then a scaling analysis should be applicable. Such a scaling analysis generally exploits the fact that for a continuous random distribution it is assumed that $R_{ij}^3 x$ is constant, where R_{ij} denotes a typical distance between the ions. Implementation of this expression in a model for spin-glass freezing, given a known functional form for the radial dependence of the exchange interaction, then yields a theoretical prediction for $T_f(x)$ which can be compared with experimental data.

This procedure was successfully used for Mn-based DMS's,[2,3,13] where T_f was found to obey the relation

$$\ln T_f \sim (n/3)\ln x \ .$$

This is compatible with a radial dependence of the exchange interaction between Mn ions of the type: $J(R)\sim R^{-n}$, where $n=6.8$ for wide gap materials as $Cd_{1-x}Mn_xTe$ or $Zn_{1-x}Mn_xSe$ and $n=5$ for lower gap materials ($Hg_{1-x}Mn_xTe$ and $Hg_{1-x}Mn_xSe$).[3] We performed a similar procedure for our data as shown in Fig. 3, where we also inserted all the available data for other Fe-based DMS's.[10] The exponent n deduced from Fig. 3 is $n\simeq 12$, indicating a much shorter range of interaction between Fe ions than observed in the Mn case. We should stress however that this result can be considered only as an indication of the possible difference in interaction range for Fe and Mn ions, since the data available up till now are too limited. We will return to this point in the Discussion.

B. High-temperature susceptibility

The high-temperature susceptibility of $Zn_{1-x}Fe_xSe$ was recently studied by us[11] in order to compare the experimental data with a high-temperature series expansion (HTE) derived for Fe^{2+}. The susceptibility was found to obey a Curie-Weiss law in the temperature range 70–300

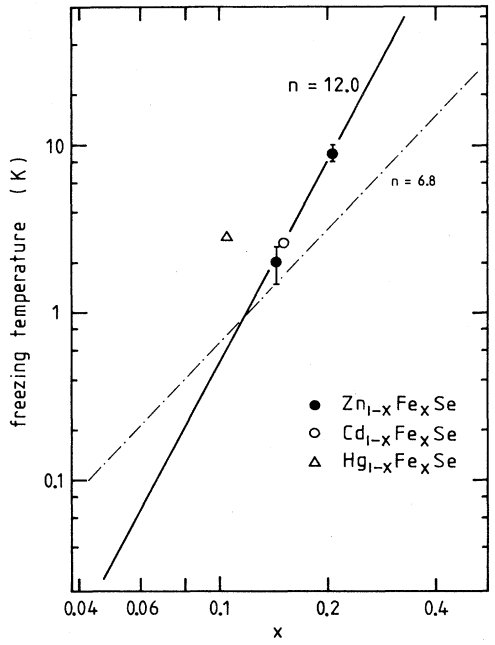

FIG. 3. Freezing temperature as a function of concentration x for $Zn_{1-x}Fe_xSe$, $Cd_{1-x}Fe_xSe$ (Ref. 10) and $Hg_{1-x}Fe_xSe$ (Ref. 10). The solid line indicates a radial decay of the exchange integral $J \sim R^{-n}$ with $n=12$; for comparison the dashed-dotted line illustrates $n=6.8$; see Ref. 3.

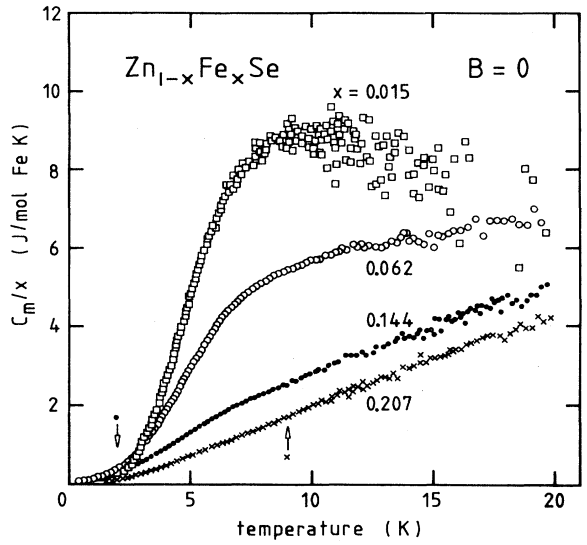

FIG. 4. Magnetic specific heat of $Zn_{1-x}Fe_xSe$ in the absence of magnetic field. The arrows indicate the freezing temperatures T_f.

K, with a negative Curie-Weiss temperature indicating antiferromagnetic coupling between Fe^{2+} ions. Based on these results we evaluated the nearest-neighbor exchange integral $J_{NN}=-22$ K, which is substantially larger than in $Zn_{1-x}Mn_xSe$ [-12.6 K (Ref. 14)]. Such a strong exchange interaction seems compatible with the freezing temperature $T_f=9$ K for $Zn_{0.79}Fe_{0.21}Se$ which is twice as large as that observed[3] in $Zn_{1-x}Mn_xSe$ with similar concentration x. We will return to the detailed analysis of the susceptibility for both low and high temperatures later on.

C. Specific heat

Specific-heat data were obtained with a conventional adiabatic heat-pulse calorimeter in the temperature range 0.4–20 K. The magnetic contribution C_m to the specific heat was obtained by subtraction of the lattice contribution of pure ZnSe. The results for C_m (per mol Fe) in zero external magnetic field are shown in Fig. 4. As quoted earlier, no anomaly was observed at the temperature T_f as indicated by arrows in the figure. The overall behavior of C_m resembles a Shottky-type anomaly for the lowest concentrations for which a well pronounced, broad maximum is observed at about 10 K. For $x>0.14$ no maximum is observed and C_m is practically a linear function of the temperature. In distinction to the Mn-based DMS's,[15,16,3,17] no structure is observed below 2 K: C_m tends to zero monotonously with decreasing temperature. No additional contribution at lower temperatures is expected since in the measured range already $\sim 87\%$ of the entropy of the ten-level system is recovered for $x=0.015$ (assuming $C_p \sim T^{-2}$ for $T>20$ K).

The decrease of C_m/x with x indicates the relevance of the Fe^{2+}-Fe^{2+} interaction. If the only contribution to C_m would be from single (isolated) ions, as proposed previously,[8] C_m would scale with x. We found that the specific heat is not appreciably influenced by a magnetic field as shown in Fig. 5: only a very slight shift of C_m to higher temperatures, hardly exceeding the experimental accuracy, can be observed. Such a behavior is again in contrast with results reported for manganese DMS's.[3,15]

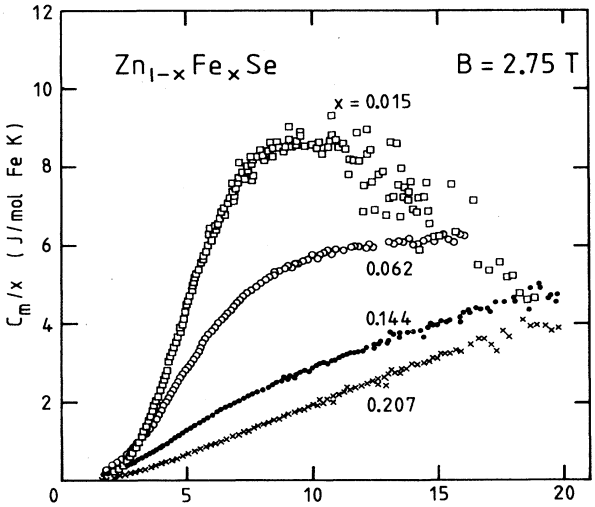

FIG. 5. Magnetic specific heat of $Zn_{1-x}Fe_xSe$ for $B=2.75$ T.

D. Magnetization

The magnetization has been measured up to 15 T and was reported earlier by one of the present authors.[8] For comparison, some relevant results will be shown later on.

III. THEORY

Very recently we proposed a model to describe the thermodynamic properties of Fe-based DMS's.[9] We will recall here the general idea behind this model and discuss it in some detail for $Zn_{1-x}Fe_xSe$. We start by considering the Fe^{2+}-Fe^{2+} pair problem.

The Hamiltonian of an Fe-Fe pair, taking into account crystal field, spin-orbit interaction, magnetic field, and exchange interaction between the Fe^{2+} ions, which is assumed to be isotropic and Heisenberg-type, can be expressed in the following form:

$$\mathcal{H}=\mathcal{H}_{CF}+\mathcal{H}_{so}+\mathcal{H}_{exch}+\mathcal{H}_B \ , \tag{1}$$

where

$$\mathcal{H}_{exch}=-2J\mathbf{S}_1\cdot\mathbf{S}_2 \ ,$$

$$\mathcal{H}_{so}=\lambda\mathbf{S}_1\cdot\mathbf{L}_1+\lambda\mathbf{S}_2\cdot\mathbf{L}_2 \ ,$$

$$\mathcal{H}_B=(\mathbf{L}_1+\mathbf{L}_2+2\mathbf{S}_1+2\mathbf{S}_2)\cdot\mu_B\mathbf{B} \ ,$$

and $\mathcal{H}_{CF}$ is the crystal-field term. J is the exchange constant,[18] $\mathbf{S}$ and $\mathbf{L}$ are spin and orbital momentum operators, respectively. The indices i and j refer to the ions of the pair.

The full Fe^{2+}-Fe^{2+} pair wave function is taken as a linear combination of products of single-ion wave functions

$$\psi=\sum_{n,m}\alpha_{nm}f_n(1)g_m(2) \ , \tag{2}$$

where $f_n(1)$ and $g_m(2)$ are single-ion wave functions. Since ^5E and ^5T terms are 10-fold and 15-fold degenerate, respectively, we are dealing finally with 625 pair basis functions. To simplify the problem, we have chosen $f_n(1)$ and $g_m(2)$ according to Slack *et al.* (wave functions $A8$ in Ref. 5). These wave functions diagonalize $\mathcal{H}_{CF}$ and $\mathcal{H}_{so}$, which means that our Hilbert space is split into four subspaces: $^5E\times{}^5E$, $^5E\times{}^5T$, $^5T\times{}^5E$, and $^5T\times{}^5T$. In all wide gap materials used as host lattices for DMS's, the crystal-field splitting is of the order of 3000 cm^{-1} and is much larger than the other terms in Hamiltonian (1) (typically 2 orders of magnitude). It is therefore reasonable to limit our considerations to the $^5E\times{}^5E$ subspace. In fact, such a limitation means that we neglect ^5E-^5T mixing caused by $\mathcal{H}_{exch}$ and $\mathcal{H}_B$. We have checked that even for very strong exchange interactions (as $J=-200$ K) the corrections to the energies resulting from this limitation do not exceed a few percent. Mixing due to spin-orbit interaction and crystal field is taken into account exactly by suitable choice of the single-ion wave functions.[19] Within the $^5E\times{}^5E$ subspace the Hamiltonian (1) is solved numerically by diagonalization of the corresponding 100×100 Hamiltonian matrix. The resulting energy pair diagram is shown in Fig. 6 for some values of J. For the crystal-field splitting and spin-orbit parameter, we adopted the values reported[6] for ZnSe:Fe ($Dq=293$ cm^{-1}, $\lambda=-85$ cm^{-1}). To demonstrate the influence of the spin-orbit coupling, the energy levels for $\lambda=-103$ cm^{-1} (i.e., the free ion value) are also shown in Fig. 6(b). It can be noticed that the exchange interaction does not essentially change the iron energy level structure, in the sense that the ground state is still a singlet one. However, the first excited state approaches the ground state when J increases. In the presence of a magnetic field, the degeneracy of the Fe^{2+}-Fe^{2+} pair is lifted as shown in Fig. 7 for fields up to 20 T.

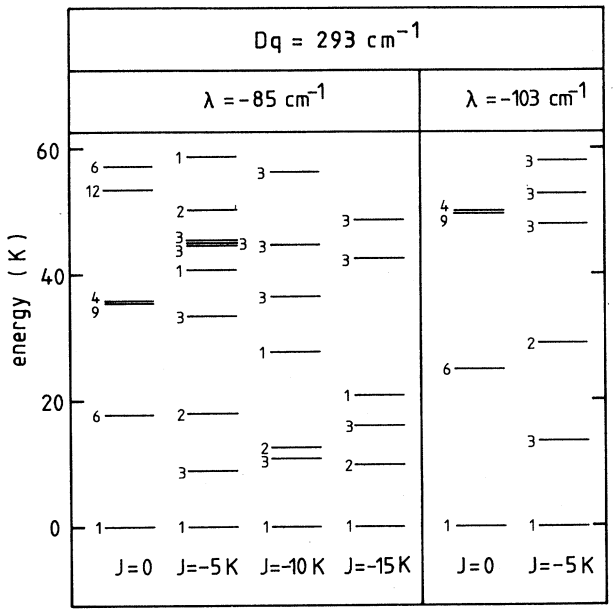

FIG. 6. Low-lying energy levels for a single Fe^{2+} ion ($J=0$) and pairs of Fe^{2+} ions with exchange interactions $J=-5$ K, $J=-10$ K, and $J=-15$ K for (a) $Dq=293$ cm^{-1} and $\lambda=-85$ cm^{-1}, (b) $Dq=293$ cm^{-1} and $\lambda=-103$ cm^{-1} (i.e., free-ion value). The numbers denote the degeneracy of the levels.

The energy level scheme can be used for the calculation of all thermodynamic properties of an Fe^{2+}-Fe^{2+} pair. In Fig. 8 we show the specific heat of a pair for different exchange interactions. For all presented J values, at low temperatures a well-pronounced maximum in the specific heat is observed, similarly to a single Fe^{2+} ion ($J=0$). This maximum shifts to lower temperatures as the exchange interaction increases and slightly changes its shape. Application of moderate magnetic fields influences the specific heat only slightly (less than 5% for $B<6$ T), which is a consequence of the small changes of the energy level separations with magnetic field (cf. Fig. 7).

In Fig. 9 the calculated magnetization of a Fe^{2+}-Fe^{2+} pair is shown for different temperatures. In distinction to the free Fe^{2+} ion magnetization (Fig. 9, inset), the pair magnetization shows no saturation with magnetic field (we checked it up to 60 T). Moreover, no characteristic steps are observed, which occur for Mn^{2+}-Mn^{2+} pairs[20–22] and are due to crossings of excited pair levels with the ground state. In the present case the ground

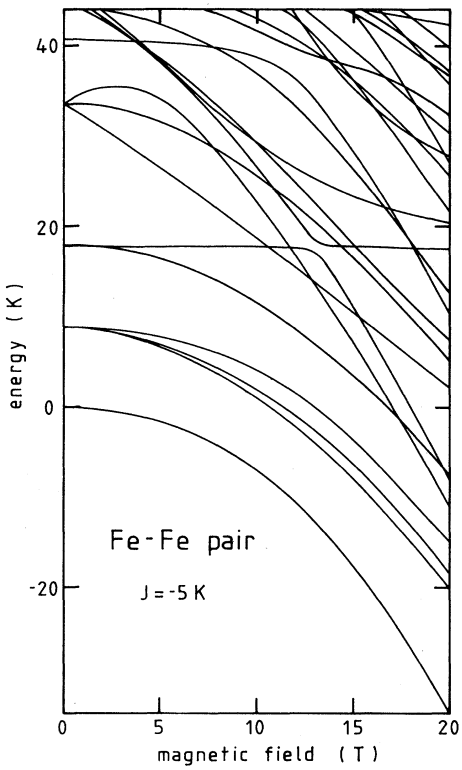

FIG. 7. Splitting of the pair energy levels in magnetic field ($J=-5$ K, $Dq=293$ cm^{-1}, and $\lambda=-85$ cm^{-1}).

state is coupled to the excited states by the magnetic field and is then pushed down instead of being crossed by excited states (Fig. 7). Therefore, no steps are predicted even at very low temperatures.

Finally, in Fig. 10 the susceptibility as a function of temperature is shown. A typical Curie-Weiss behavior

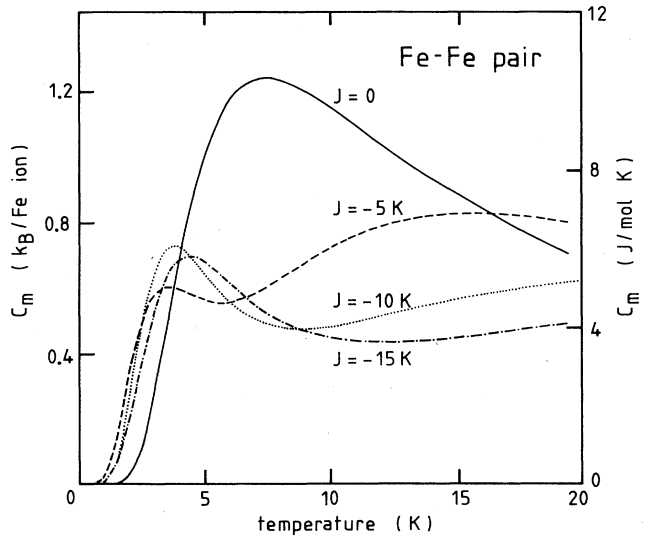

FIG. 8. Specific heat of a Fe^{2+}-Fe^{2+} pair as a function of temperature for $J=-5$, -10, and -15 K ($Dq=293$ cm^{-1}, $\lambda=-85$ cm^{-1}) in the absence of a magnetic field. For comparison the behavior for noninteracting ions ($J=0$) is also shown.

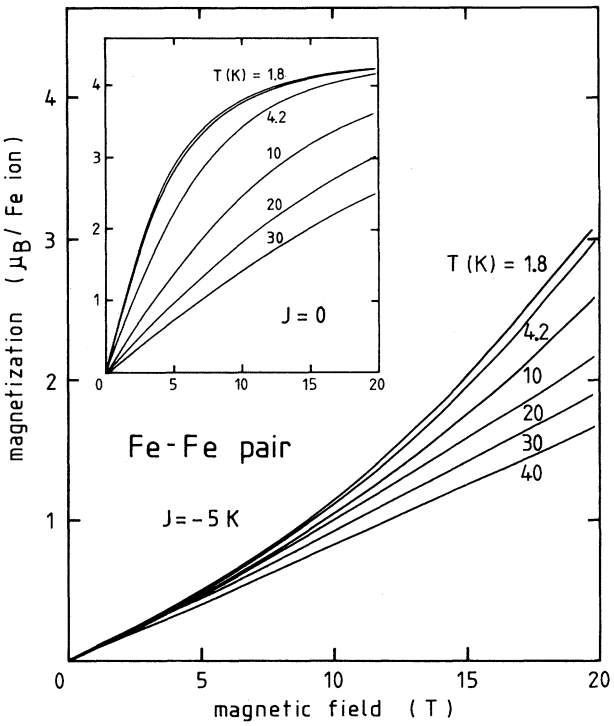

FIG. 9. Magnetization of a Fe^{2+}-Fe^{2+} pair coupled by an exchange interaction $J=-5$ K as a function of magnetic field for different temperatures ($Dq=293$ cm^{-1}, $\lambda=-85$ cm^{-1}). Inset: magnetization of a single, isolated Fe^{2+} ion ($J=0$) as a function of temperature for the same parameters Dq and λ.

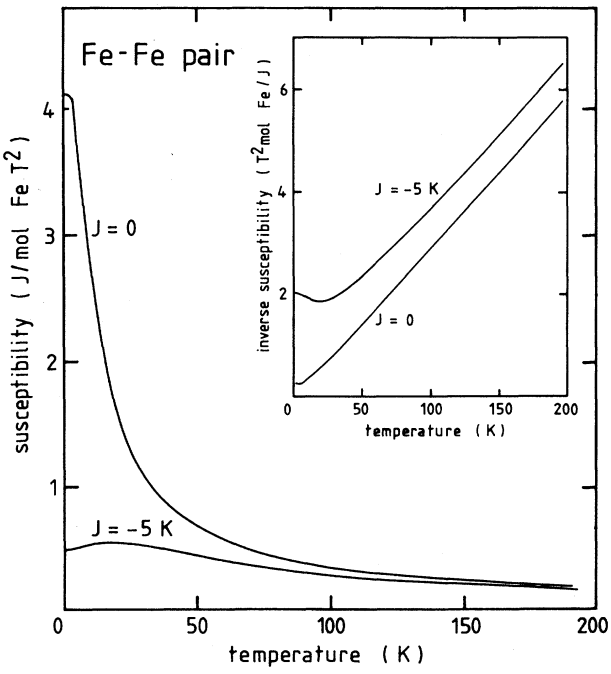

FIG. 10. Susceptibility of a Fe^{2+}-Fe^{2+} pair coupled by an exchange interaction $J=-5$ K as a function of temperature ($Dq=293$ cm^{-1}, $\lambda=-85$ cm^{-1}). For comparison the behavior of noninteracting ions ($J=0$) is also shown. Inset: inverse susceptibility as a function of temperature.

$[\chi \sim (T-\Theta)^{-1}]$ is predicted for the high-temperature limit when an interaction is present in distinction to the Curie-type behavior ($\chi \sim T^{-1}$) for a single Fe ion in a crystal field.

IV. INTERPRETATION

Using the results of the preceding section, one can now describe the relevant thermodynamic properties of a "real" $Zn_{1-x}Fe_xSe$ crystal in the so-called extended nearest-neighbor pair approximation (ENNPA),[23] which was recently successfully used for description of the magnetic properties of Mn-based DMS's.[13,3]

ENNPA is an approximative calculation method particularly useful for random, diluted systems with long-ranged interactions. It is based on the assumption that the partition function of the whole crystal can be factorized into contributions of pairs of ions. In this method each ion is considered to be coupled by an exchange interaction J_i only to its nearest magnetic neighbor, which may be located anywhere at a distance R_i. The statistical weight of pair configurations with different R_i is given by random distribution of the magnetic ions, and therefore any thermodynamic quantity can be expressed in the following form:

$$A = \sum_i A_i(J_i) P_i(x)/2 \ , \tag{3}$$

where A_i represents the specific heat, susceptibility, or magnetization of a pair and depends on J_i. $P_i(x)$ is the probability of finding at least one nearest Fe ion in the ith shell and corresponds for a random distribution to

$$P_i(x) = (1-x)^{n_{i-1}} - (1-x)^{n_i} \ , \tag{4}$$

where n_i is the number of lattice sites inside a shell of radius R_i. For the actual calculations we have to insert values for the parameters: Dq, λ, J_1, J_2, J_3, ... For the crystal-field splitting and spin-orbit parameters, we have taken the values $\Delta = 2930\ \text{cm}^{-1}$ (or $Dq = 293\ \text{cm}^{-1}$) and $\lambda = -85\ \text{cm}^{-1}$ reported[6] for ZnSe doped with Fe. These values result from combining spectroscopic data for the ${}^5E \rightarrow {}^5T$ optical transition[24] with susceptibility results,[6] assuming Ham's reduction factor[25] to equal 1. We notice that the crystal-field parameter obtained in that way is practically determined by the energy of the ${}^5E \rightarrow {}^5T$ transition, since it depends only very weakly on the value of λ (20% variation of λ results in 1% variation of Δ), whereas the spin-orbit parameter results from the fitting procedure. The exchange integral for nearest neighbors is provided by recent high-temperature susceptibility data[11]: $J_{NN} = -22$ K. The interaction range is suggested to be $J_i = J_{NN} R^{-12}$ (see Sec. II). This means, in practice, that only the nearest-neighbor interaction is relevant, since more distant neighbors are so weakly coupled that their magnetic properties differ very little from those of single ions. However, as we already discussed in Sec. II, the data concerning the spin-glass freezing in Fe-based DMS's are not sufficient to provide reliable information about this interaction range. We will therefore discuss two cases: only nearest neighbor, short-ranged interaction (NN), and a long-range interaction (LR), assuming the same interaction range as reported[3] for $Zn_{1-x}Mn_xSe$ ($J_i = J_{NN} R^{-6.8}$).

The ENNPA calculations were performed numerically. The summation over i shells in (3) was carried out up until $i = v$ for which

$$\sum_{i=1}^{v} P_i(x) > 0.99 \ . \tag{5}$$

In practice $v = 12$ was quite sufficient for all x.

The calculated specific heat, together with the experimental data, is shown in Fig. 11 for $x = 0.015$, and Fig. 12 for $x = 0.062$. It is obvious that, if the exchange interaction between the Fe ions is taken into account, a much better description of the experimental data can be obtained than for the noninteracting ion model ($J = 0$ in Figs. 11 and 12). The latter description is reasonable for $x = 0.015$, whereas a substantial discrepancy is found for $x = 0.062$. We should note, however, that the dilute limit which is essential in the ENNPA may not be satisfied for $x = 0.06$. In fact, for Mn-based DMS's, only crystals containing less than 5% magnetic ions could be properly described by the ENNPA.[13,3]

In the dilute limit, where the single-ion contribution is dominant, the exponential onset of C_m clearly marks the influence of the energy gap between the ground state and the first-excited state. The systematic deviation of the calculations from the experimental data in the low-temperature region indicates that the actual lowest energy gap is somewhat larger than that resulting from the parameters taken in the present calculation (~ 18 K). An

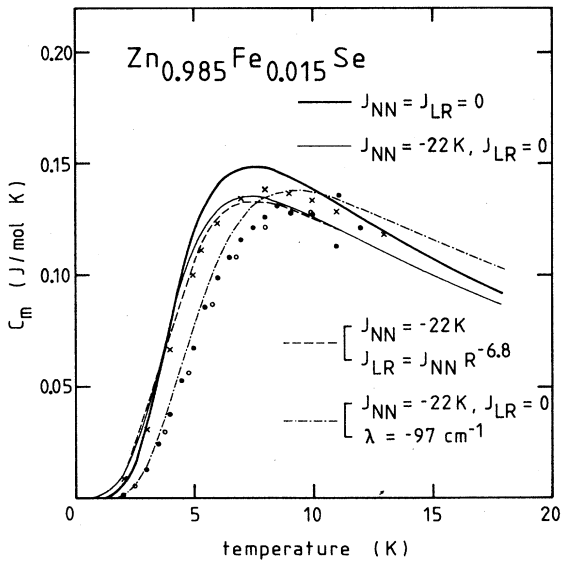

FIG. 11. Specific heat of $Zn_{0.985}Fe_{0.015}Se$ in the ENNPA as a function of temperature in the absence of a magnetic field for $Dq = 293\ \text{cm}^{-1}$, $\lambda = -85\ \text{cm}^{-1}$, and various exchange interaction parameters. The crosses show the influence of a magnetic field $B = 2.64$ T for $J_{NN} = -22$ K and $J_{LR} = 0$. Also the influence of a different spin-orbit parameter, $\lambda = -97\ \text{cm}^{-1}$, is shown. The points represent experimental data: solid circles $B = 0$, open circles $B = 2.75$ T.

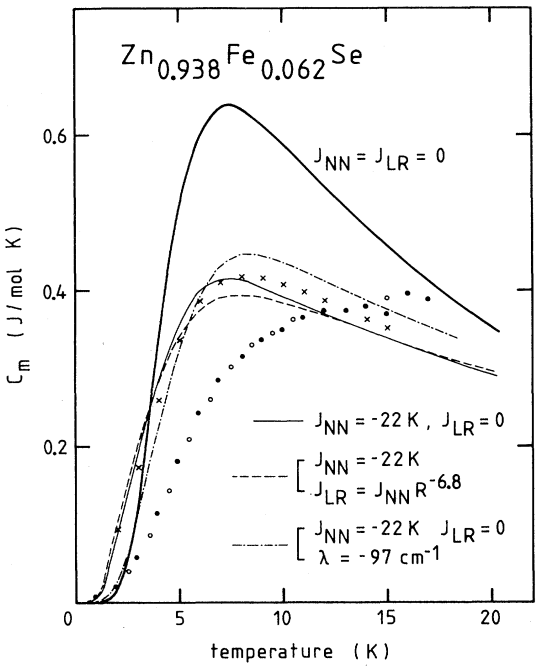

FIG. 12. Specific heat of $Zn_{0.938}Fe_{0.062}Se$ in the ENNPA as a function of temperature in the absence of a magnetic field for $Dq=293$ cm^{-1}, $\lambda=-85$ cm^{-1}, and various exchange interaction parameters. The crosses show the influence of a magnetic field $B=2.64$ T for $J_{NN}=-22$ K and $J_{LR}=0$. Also the influence of a different spin-orbit parameter, $\lambda=-97$ cm^{-1}, is shown. The points represent experimental data: solid circles $B=0$, open circles $B=2.75$ T.

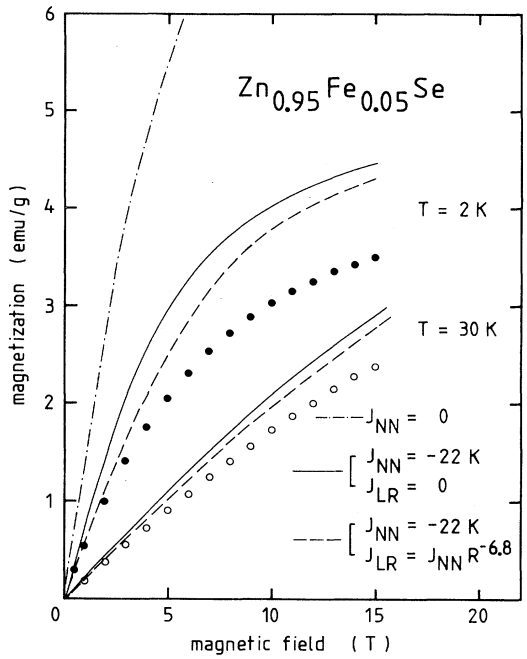

FIG. 13. Magnetization of $Zn_{0.95}Fe_{0.05}Se$ in the ENNPA as a function of magnetic field at $T=2$ and 30 K for $Dq=293$ cm^{-1}, $\lambda=-85$ cm^{-1}, and various exchange interaction parameters. The points represent experimental data (Ref. 8).

increase of this gap to ~ 22 K is necessary to explain the observed specific heat. Preliminary far-infrared transmission (FIR) experiments,[26] where we observed the optical transitions $A_1 \rightarrow T_1$ and $A_1 \rightarrow T_2$, have confirmed this suggestion. To explain the experimental $E(T_1)-E(A_1)$ and $E(T_2)-E(A_1)$ energy differences within the framework of Slack's model,[5] one has to adjust the spin-orbit parameter to -97 cm^{-1} keeping Dq unchanged. The resulting specific heat is shown in Figs. 11 and 12. One can notice that this larger value of λ indeed improves the description, although, especially for the higher concentration, significant deviations remain.

High-field magnetization results are shown in Fig. 13 for $Zn_{0.95}Fe_{0.05}Se$. Also in this case it is evident that ion-ion interactions have to be taken into account.

The magnetic susceptibility calculations are presented in Fig. 14 for $Zn_{0.978}Fe_{0.022}Se$ and $Zn_{0.928}Fe_{0.072}Se$.[11] The typical curvature of the calculated susceptibility, which is also observed in the experimental data, is obviously due to exchange interactions and is neither observed for semi-isolated Fe^{2+} ions,[6] nor produced by calculations for isolated ions as shown in Fig. 14 ($J=0$). Again we observe an increasing discrepancy between calculations and experimental data when the concentration increases.

For all magnetic properties considered here, we observe (cf. Figs. 11–14) that the difference between calculations in which the exchange interaction is implemented by the nearest neighbors alone, or by a long-range interaction $J(R)$, is not very significant. This results from the fact, as we quoted before,[9] that the further neighbors exchange interactions, are too weak to alter the Fe^{2+} level scheme significantly. Consequently, no pertinent conclusions about the interaction range can be drawn from

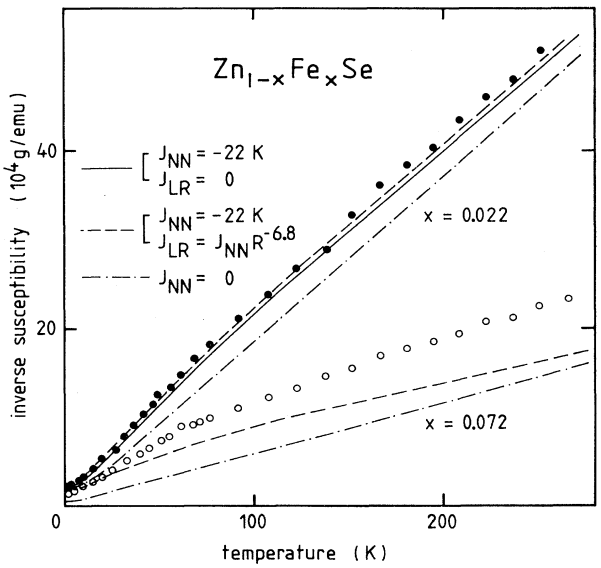

FIG. 14. Inverse susceptibility of $Zn_{1-x}Fe_xSe$ for $x=0.022$ and $x=0.072$ in the ENNPA as a function of temperature for $Dq=293$ cm^{-1}, $\lambda=-85$ cm^{-1}, and different exchange interaction parameters. The points represent experimental data (Ref. 11).

the present data.

Summarizing the present results we feel that the model presented earlier provides a reasonable, simultaneous description of all the magnetic properties with a single set of parameters. We believe that the observed deviations at higher Fe concentrations are mainly due to the fact that these concentrations are somewhat outside the diluted limit, to which the ENNPA is specifically applicable.

We would like to emphasize that no fitting parameters are employed in our calculations and comparison with the data. Such a procedure would certainly yield a better description of some of the experimental data, but, in view of the large number of parameters, it would not be necessarily physically meaningful.

V. DISCUSSION AND CONCLUSIONS

As quoted earlier, specific-heat data and preliminary FIR experiments indicated that the energy gap between the ground state and the first-excited states is somewhat larger than the calculated gap resulting from the reported crystal-field and spin-orbit parameters. To describe this splitting within Slack's model, the spin-orbit coupling parameter had to increase from $-85\ \mathrm{cm}^{-1}$ to $-97\ \mathrm{cm}^{-1}$. One has to note however that this is just a formal description. Physically, it seems more likely that substitution of magnetic ions results in a local lowering of the cubic symmetry which may lift the orbital degeneracy to start with. However, data to support this conjecture are not available and we therefore refrained from implementing these effects.

Furthermore, we would like to point out that our use of an isotropic exchange interaction term of the Heisenberg type must be considered as a first approximation. Generally speaking, anisotropic terms will be present for Fe^{2+}-Fe^{2+} interactions, specifically when the actual calculations are restricted (as in the present case) to the lower subset of levels.

Finally, we would like to comment on the exchange interaction between Fe^{2+} ions in relation to Mn^{2+}-Mn^{2+} exchange. In Table I we collected the available data concerning Fe and Mn exchange in similar DMS's. Inspection of this table shows that no drastic differences are observed between Mn and Fe exchange. An antiferromagnetic, long-range exchange is found in all cases, although the nearest-neighbor interaction is stronger for Fe and seems to be of shorter range than for Mn. Assuming that superexchange is the dominant mechanism, as was rather well established for Mn-type DMS's, the simultaneous increase of strength and decrease of range is not completely in accordance with theory. In general, an increasing strength is expected to be accompanied with an increasing range[31] or the range is considered as largely independent of the atomic constituents.[32] These tendencies, however, mainly refer to comparisons between Mn-type DMS's. The substitution of Fe instead of Mn may well result in changes in the band structure and d energy levels, which complicate a meaningful comparison since both the location of the unoccupied d levels with respect to the valence band, as well as the degree of hybridization determine the strength of J_{NN}, at least for the first few neighbors.[31,32] Although calculations of Wei *et al.*[33] seem to indicate an increase of the hybridization for Fe^{2+} (or Mn^{+}), which would be consistent with the observed increase of J_{NN} as well as the p-d exchange parameter N_0 (cf. Table I), we feel that pertinent conclusions would be rather speculative at the present stage.

With respect to the range of the long-range interaction ($\sim 1/n$), as probed by the freezing temperature as a function of x, a comment must be made. The relation between T_f and concentration x is based on a scaling analysis and the conjecture that T_f is related to the interaction energy at the average distance ($\bar{R}$) between the magnetic ions,[3] e.g.,

$$k_B T_F \simeq J(\bar{R}) S^2 \ . \tag{6}$$

In the case that we are dealing with a singlet ground state with a quenched magnetic moment, the interaction energy is less effective and should be modified, implementing the fact that the interacting ions have only an induced moment. This situation is somewhat analogous to the case studied by Moriya[34] who showed, in a mean field approximation, that an ensemble of Ni^{2+} ions with singlet ground state cannot sustain spontaneous order unless the exchange interaction is, roughly speaking, strong enough to overcome the ground-state splitting.

We will illustrate this behavior by considering the pair correlation function $\langle \mathbf{S}_1 \cdot \mathbf{S}_2 \rangle$ for $S=2$ ions both with and without a singlet ground state coupled with an exchange interaction $J\mathbf{S}_1 \cdot \mathbf{S}_2$. The Hamiltonian is written as

$$\mathcal{H}_{12} = -2J\mathbf{S}_1 \cdot \mathbf{S}_2 + D(S_{1z}^2 + S_{2z}^2) + \frac{E}{2}(S_{1x}^2 - S_{1y}^2 + S_{2x}^2 - S_{2y}^2) \ . \tag{7}$$

TABLE I. Nearest-neighbor interaction strength (J_{NN}), radial dependence of the interaction (n with $J \sim R^{-n}$), and p-d exchange parameter (N_0) for several Mn- and Fe-type DMS's.

	Mn			Fe		
	J_{NN} (K)	n	N_0 (eV)	J_{NN} (K)	n	N_0 (eV)
CdSe	-10[a]	6.8[c]	-1.27[e]	-18[g,h]		
ZnSe	-12.6[a]	6.8[c]	-1.30[f]	-22[h]	12	-1.6[i]
ZnS	-16[b]	7.6[d]				

[a] Reference 28.
[b] Reference 14.
[c] Reference 3.
[d] Reference 17.
[e] Reference 27.
[f] Reference 29.
[g] Reference 10.
[h] Reference 11.
[i] Reference 30.

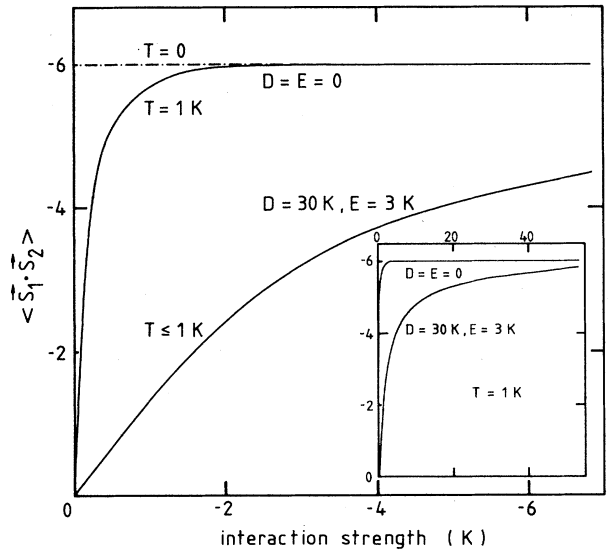

FIG. 15. Calculated low-temperature pair correlation function $\langle \mathbf{S}_1 \cdot \mathbf{S}_2 \rangle$, for Hamiltonian (7) with $S=2$, as a function of interaction strength J. Two cases are considered, i.e., the degenerate ($D=E=0$) and the singlet single-ion ground state ($D \neq 0$, $E \neq 0$). In the latter case the energy splitting between ground and first-excited state equals 22 K.

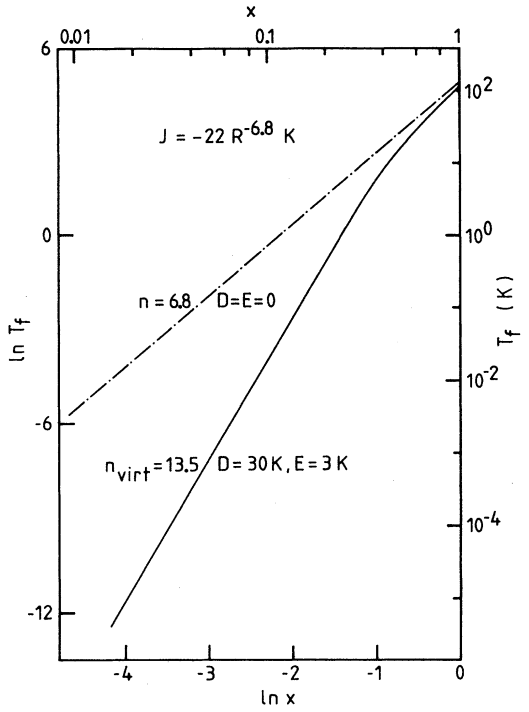

FIG. 16. Calculated freezing temperature T_f as a function of the concentration x on a logarithmic scale, using $k_B T_f = J(R)\langle \mathbf{S}_0 \cdot \mathbf{S}_{\bar{R}} \rangle$ and $J(R) = -22R^{-6.8}$ K, $R = \bar{R}/R_{\mathrm{NN}} = (1/x)^{1/3}$; see Fig. 15 ($T=0$).

The singlet ground state of the individual ions is created by allowing D and E to be nonzero. For zero D, E a degenerate ground state of the ions is obtained. Figure 15 shows the calculated pair correlation function $\langle \mathbf{S}_1 \cdot \mathbf{S}_2 \rangle$ for the two cases at low temperatures, as a function of J. D and E are chosen such that an energy-level scheme is obtained with a splitting between ground state and first-excited state similar to that observed in $Zn_{1-x}Fe_xSe$. From Fig. 15 it is clear that the pair correlation for coupled ions with singlet ground states depends on J and is appreciably smaller than the pair correlation for coupled ions with a degenerate ground state, at least for small J. Now we have to realize that actually the interaction energy in Eq. (6) must be written as proportional to $J\langle \mathbf{S}_1 \cdot \mathbf{S}_2 \rangle$, which, as can be seen from Fig. 15, approaches the value $-JS(S+1)$ in the fully aligned limit. If we perform an analysis on the concentration dependence[3] of T_f, using the pair exchange energy $J(\bar{R})\langle \mathbf{S}_0 \cdot \mathbf{S}_{\bar{R}} \rangle$ following from the preceding calculations, the resulting $T_f(x)$ does not necessarily reveal the radial dependence of $J(R)$. This is illustrated in Fig. 16 where the calculated results for $T_f(x)$ are shown obtained for the two cases considered in Fig. 15. For both cases, the same radial dependence of $J(\bar{R})$ is used: $J \sim R^{-6.8}$. For the pairs with the degenerate ground state, the resulting $T_f(x)$ indeed shows the implemented range of interaction $(1/n)$. However, for pairs with a singlet ground state, the range, as probed by $T_f(x)$, is virtually suppressed due to the reduction of $\langle \mathbf{S}_1 \cdot \mathbf{S}_2 \rangle$ for small J, yielding $n \simeq 13.5$ instead of $n = 6.8$. Although the actual energy-level scheme of Fe^{2+} in $Zn_{1-x}Fe_xSe$ is much more complicated than considered in this simple illustration, it is surprising to note that this virtual range of interaction ($n \sim 13.5$) is rather close to the range actually observed from the experimental data ($n \simeq 12$).

ACKNOWLEDGMENTS

We wish to thank T. F. H. v. d. Wetering, C. v. d. Steen, P. J. H. Bloemen, and H. J. M. Heyligers for their considerable help in collecting the data and performing the numerous calculations. The authors gratefully acknowledge helpful discussions with J. A. Gaj and K. Kopinga. Part of this work was carried out under the Polish Central Project for Fundamental Research No. CPBP 01.06 and the Foundation for Fundamental Research on Matter (FOM) that forms part of the Netherlands Organization for the Advancement of Research (NWO). One of us (A.T.) wishes to express his gratitude for the hospitality during his stay at Eindhoven.

*On leave from the Institute of Experimental Physics, The University of Warsaw, Hoza 69, PL-00-681 Warsaw, Poland.

[1]See review papers: S. von Molnar, Mat. Res. Soc. Symp. Proc. **89**, 39 (1987); N. B. Brandt and V. V. Moshalkov, Adv. Phys. **33**, 193 (1984); J. K. Furdyna, J. Appl. Phys. **53**, 8637 (1982); J. A. Gaj, J. Phys. Soc. Jpn. Suppl. **49**, A797 (1980).

[2]W. J. M. de Jonge, A. Twardowski, and C. J. M. Denissen, Mat. Res. Soc. Symp. Proc. **89**, 156 (1987).

[3]A. Twardowski, H. J. M. Swagten, W. J. M. de Jonge, and M. Demianiuk, Phys. Rev. B **36**, 7013 (1987).

[4]W. Low and M. Weger, Phys. Rev. **118**, 1119 (1960).

[5]G. A. Slack, S. Roberts, and J. T. Wallin, Phys. Rev. **187**, 511 (1969).

[6]J. P. Mahoney, C. C. Lin, W. H. Brumage, and F. Dorman, J. Chem. Phys. **53**, 4286 (1970).

[7]See the review paper A. Mycielski, Mat. Res. Soc. Symp. Proc. **89**, 159 (1987).

[8]A. Twardowski, M. von Ortenberg, and M. Demianiuk, J. Cryst. Growth **72**, 401 (1985).

[9]A. Twardowski, H. J. M. Swagten, T. F. H. v. d. Wetering, and W. J. M. de Jonge, Solid State Commun. **65**, 235 (1988).

[10]A. Lewicki, J. Spałek, and A. Mycielski, J. Phys. C **20**, 2005 (1987).

[11]A. Twardowski, A. Lewicki, M. Arciszewska, W. J. M. de Jonge, H. J. M. Swagten, and M. Demianiuk, Phys. Rev. B **38**, 10 749 (1988).

[12]B. T. Jonker, J. J. Krebs, S. B. Qadri, and G. A. Prinz, Appl. Phys. Lett. **50**, 848 (1987).

[13]C. J. M. Denissen, H. Nishihara, J. C. van Gool, and W. J. M. de Jonge, Phys. Rev. B **33**, 7637 (1986).

[14]T. M. Giebultowicz, J. J. Rhyne, and J. K. Furdyna, J. Appl. Phys. **61**, 3537 (1987); **61**, 3540 (1987).

[15]R. R. Gałązka, S. Nagata, and P. H. Keesom, Phys. Rev. B **22**, 3344 (1980); S. Nagata, R. R. Gałązka, D. P. Mullin, H. Arbarzadeh, G. D. Khattak, J. K. Furdyna, and P. H. Keesom, *ibid.* **22**, 3331 (1980).

[16]C. D. Amarasekara, R. R. Gałązka, Y. Q. Yang, and P. H. Keesom, Phys. Rev. B **27**, 2868 (1983).

[17]H. J. M. Swagten, A. Twardowski, W. J. M. de Jonge, M. Demianiuk, and J. K. Furdyna, Solid State Commun. **66**, 791 (1988).

[18]We neglected here a possible pseudodipolar exchange interaction which was, in general, considered in Ref. 9, since no information is provided about it.

[19]In our previous paper (Ref. 9) we used a simpler basis, given by Slack *et al.* (Ref. 5) in their Tables VIII and IX. In that way ^5E-^5T mixing due to $\mathcal{H}_{so}$ was treated in second-order perturbation method. It should be stressed, however, that no substantial difference was found between present and the later results.

[20]R. L. Aggarwal, S. N. Jasperson, Y. Shapira, S. Foner, T. Sakibara, T. Goto, N. Miura, K. Dwight, and A. Wold, in *Proceedings of the 17th International Conference on the Physics of Semiconductors, San Francisco, 1984,* edited by J. D. Chadi and W. A. Harrison (Springer, New York, 1985), p. 1419.

[21]Y. Shapira, S. Foner, D. H. Ridgley, K. Dwight, and A. Wold, Phys. Rev. B **30**, 4021 (1984).

[22]J. P. Lascaray, M. Nawrocki, J. M. Broto, M. Rakoto, and M. Demianiuk, Solid State Commun. **61**, 401 (1987).

[23]K. Matho, J. Low Temp. Phys. **35**, 165 (1979).

[24]J. M. Baranowski, J. W. Allen, and G. L. Pearson, Phys. Rev. **160**, 627 (1967).

[25]F. S. Ham, Phys. Rev. **138**, A1727 (1965).

[26]A. Twardowski, H. J. M. Swagten, and W. J. M. de Jonge, in Proceedings of the 19th International Conference on the Physics of Semiconductors, 1988, Warsaw, Poland (unpublished).

[27]M. Arciszewska and M. Nawrocki, J. Phys. Chem. Solids **47**, 309 (1986).

[28]J. Spałek, A. Lewicki, Z. Tarnawski, J. K. Furdyna, R. R. Gałązka, and Z. Obuszko, Phys. Rev. B **33**, 3407 (1986).

[29]A. Twardowski, M. von Ortenberg, M. Demianiuk, and R. Pauthenet, Solid State Commun. **51**, 849 (1984).

[30]A. Twardowski, P. Glod, W. J. M. de Jonge, and M. Demianiuk, Solid State Commun. **64**, 63 (1987).

[31]G. A. Sawatzky, W. Geertsma, and C. Hass, J. Magn. Magn. Mater. **3**, 37 (1976); C. E. T. Goncalves da Silva and L. M. Falicov, J. Phys. C **5**, 63 (1972); A. N. Kocharyan and D. I. Khomskii, Fiz. Tverd. Tela (Leningrad) **17**, 462 (1975) [Sov. Phys.—Solid State **17**, 290 (1975)].

[32]H. Ehrenreich, K. C. Hass, B. E. Larson, and N. F. Johnson, in Mat. Res. Soc. Symp. Proc. **89**, 187 (1987); B. E. Larson, K. C. Hass, H. Ehrenreich, and A. E. Carlsson, Solid State Commun. **56**, 347 (1985).

[33]Su-Huai Wei and A. Zunger, Phys. Rev. B **35**, 2340 (1987).

[34]T. Moriya, Phys. Rev. **117**, 635 (1960).